RSC Advances

RSC Advances

www.rsc.org/advances

ROYAL SOCIETY OF CHEMISTRY

www.rsc.org/advances

RSC Advances

PAPER

Acid - vacuo heat treated low cost banana stems fiber for efficient biosorption of Hg(II)†

N. Salamun,[a] S. Triwahyono[a,b], A.A. Jalil[c,d] , T. Matsuura[e] and N.F.M. Salleh[d]

The potential of banana stem fiber (BSF) as a low cost biosorbent for Hg(II) removal was studied. HCl treatment increased the cellulose accessibility which led to enhance the interaction of Hg(II) and BSF. Activation of BSF-HCl in vacuo at 373 K increased the maximum biosorption capacity from 28 to 372 mg g^{-1} and altered the activation energy from 3.5 to 76.9 kJ mol^{-1} showing the increasing of Hg(II) chemisorption. FTIR and ESR results confirmed the large amount of structural defects on the activated BSF-HCl which led to increase the Hg(II) uptake. Batch biosorption models showed that the kinetics follow pseudo-second-order and the equilibrium uptake fitted to all three-parameter models showing the Hg(II) biosorption behaves as a Langmuir isotherm. The non-linear regression method exhibited higher coefficient of determination values for isotherm and kinetic analyses compared to linear method. The thermodynamic functions indicated that the nature of Hg(II) biosorption is exothermic and non-spontaneous process.

1. Introduction

Aqueous heavy metal pollution represents an important environmental problem due to its toxic effects and accumulation throughout the food chain. Among the heavy metals, mercury is considered as one of the most dangerous for human health. The major sources of mercury pollution are effluents from oil refining, pulp paper, chlor-alkali, pharmaceutical, electrical, rubber processing and fertilizer industries.[1-2] The most common mercury species present in natural water samples are mercury(II) and methyl mercury. The toxicity of Hg depends on the concentration and its chemical form. Therefore, the accuracy and sensitivity in the determination of mercury is very important. Several analytical methods have been developed for the determination of mercury in water such as old vapour atomic fluorescence spectrometry (CV-AFS), inductively coupled plasma optical emission spectrometry (ICP-OES) and microwave plasma atomic emissi-

on spectrometry (MP-AES).[3-6] As Hg(II) is a highly toxic element, the removal of mercury from effluents has been a significant concern in most industrial branches, due to economic and environmental factors.

In recent years, biosorption appears to be the most promising method because of its cost effective, easy regeneration of biosorbents, and possibility of metal recovery[7-9]. Several research groups have studied inexpensive naturally occurring lignocellulosic materials such as coconut coir pith, wheat straw, rice husk ash, sugarcane bagasse, tree fern, saw dust, maize and tomato peel for heavy metals removal.[10-16] Banana stem is another commonly available and abundant natural material where it is also an example of lignocellulosic biomass waste, which composed of cellulose, hemicellulose, lignin, tannin and pectin. Various chemical groups exist on the banana stem including carboxyl, hydroxyl and amide groups which have been extensively proven to play a critical role in the biosorption processes by cation/anion exchange phenomena. Although lignocellulosic biomass waste was shown to be an effective adsorbent for a wide range of metals ions, crop residues suffer from at least two major drawback; low exchange or sorption capacity and poor physical stability.[17] In order to overcome these problems, physical or chemical modifications of raw adsorbents such as comminution, milling, soaking and functionalization are required for generating more active sites.[18]

In the present work, the effects of treatments and activation of banana stem fibers on the Hg(II) biosorption were studied. The

[a]Department of Chemistry, Faculty of Science, Universiti Teknologi Malaysia, 81310 UTM Johor Bahru, Johor, Malaysia.
[b]Ibnu Sina Institute for Fundamental Science Studies, Universiti Teknologi Malaysia, 81310 UTM Johor Bahru, Johor, Malaysia.
[c]Institute of Hydrogen Economy, Universiti Teknologi Malaysia, 81310 UTM Johor Bahru, Johor, Malaysia.
[d]Department of Chemical Engineering, Faculty of Chemical Engineering, Universiti Teknologi Malaysia, 81310 UTM Johor Bahru, Johor, Malaysia.
[e]Industrial Membrane Research Laboratory, Department of Chemical and Biological Engineering, University of Ottawa, 161 Louis Pasteur St., Ottawa, ON K1N 6N5, Canada
Email: sugeng@utm.my

results showed that acid treatment and activation in vacuo at 373 K markedly increased the Hg(II) biosorption capacity of BSF. The activation increased the maximum biosorption capacity of BSF-HCl from 28 to 372 mg g^{-1} and induced the chemisorption process due to the presence of more surface defects on the biosorbent. The kinetics and thermodynamics studies indicated that the nature of Hg(II) biosorption on BSF-HCl is exothermic, non-spontaneous and adsorbed on the heterogeneous surface of biosorbent. To reduce the cost of removal process, the recovery of Hg(II) and reusability of the biosorbent using HCl as eluted solution were studied.

2. Experimental
2.1 Preparation of BSF adsorbent

BSF were extracted from the pseudostem of banana plant which was collected in Johor Bahru (Malaysia) area. The leaf sheaths from the pseudostem were ground, sieved and dried in air for a week. The lignin content in the BSF was removed by treating with H_2O_2 and hypochlorite system, followed by drying at room temperature in air. The resulting BSF was treated separately with 0.1M NaOH (Merck) and 0.1M HCl (37 %, Merck) followed by washing till the pH 7, drying overnight at 373 K and storing in a vacuum desiccator. The biosorbent was labelled as BSF-NaOH and BSF-HCl, respectively while the untreated BSF was denoted as BSF-raw.

2.2 Characterization of BSF

The cellulose, hemicellulose and lignin contents were determined using a technique described by Moubasher et al.[19] 2 g of BSF was boiled in ethanol (Merck) for 15 min, followed by washing and drying at 353 K overnight. It was again weighed and then divided into two equal parts in which one part is considered as A fraction. Second part of residue was treated with 24% KOH (Merck) for 4 h at 273 K, followed by washing and drying at 353 K and the dry weight was taken as B fraction. The same sample was further treated with 72% H_2SO_4 (Merck) for 3 h to hydrolyse the cellulose and then was refluxed with 5% H_2SO_4 for 2 h. Then the H_2SO_4 was removed by washing with distilled water. It was then dried at 353 K and the dry weight was taken as C fraction. Cellulose was calculated by the difference (B-C), hemicellulose (A-B) and lignin is C itself.

The X-ray diffraction (XRD) patterns of the biosorbents were recorded on a Bruker AXS D8 Automatic Powder Diffractometer using Cu Kα radiation with λ= 1.5418Å at 40 kV and 40 mA in the range of 2θ = 20-60°. The Segal's empirical method[20] was used to detemine the crystallinity index of the samples Xc, as shown in Eq. (1):

$$X_c = I_{002} - I_{am}/I_{002} \times 100 \qquad (1)$$

where I_{002} and I_{am} are the peak intensities of crystalline and amorphous materials, respectively.

Infrared spectra of the biosorbents were obtained using an Agilent Cary 640 FTIR Spectrometer. Prior to the analysis, the sample was outgassed at 373 K for 1 h to remove the moisture contents[21].

Thermogravimetric (TGA) analysis was carried out with a Mettler Toledo TGA/SDTA851. Approximately 8 mg sample was heated from 298 to 1073 K at 10 K min^{-1}, under flow of N_2 (20 mL min^{-1}).

Electron spin resonance (ESR) provides signals corresponding to free radicals and/or paramagnetic ions, which is a count of the number of unpaired electrons (spins) available in a sample. ESR study was conducted using a JEOL JES-FA100 ESR spectrometer at room temperature.

The zero point charge (pH_{zpc}) of the BSF was determined using a powder addition method.[22]

2.3 Biosorption experiments

Batch biosorption experiment was conducted by adding 0.01 g biosorbent in a 200 mL of 10 mg L^{-1} Hg(II) solution. The Hg(II) solution was prepared by dissolving $HgCl_2$ (Merck) in double distilled water. Prior to the biosorption, the biosorbent was activated in a vacuo at 373 K for 1 h unless otherwise specified. The pH of the working solutions was adjusted to the desired value with 0.1 M HCl or 0.1 M NaOH. The mixture was incubated with a constant stirring rate of 300 rpm at room temperature to reach equilibrium. The biosorption isotherm experiment was conducted at 303 K with the concentration varying from 5 to 200 mg L^{-1}, while the kinetic and thermodynamic experiments were conducted at 303-323 K with a constant initial Hg concentration (100 mg L^{-1}). The sampling was taken at appropriate time intervals and followed by centrifugation at 14,000 rpm for 15 min. The residual Hg(II) concentration was determined with an Agilent 4100 MP-AES spectrometer.

2.4 Desorption and regeneration tests

To investigate the possibility of repeated use of the biosorbent, desorption and regeneration experiments were also conducted. The Hg(II)-loaded BSF-HCl was filtered, and Hg(II) content in the solution was measured. The biosorbent was then transferred to another conical flask and stirred with 50 mL of 0.1 M HCl solution for 4 h. It was again filtered and the desorbed Hg(II) was determined in the filtrate. The biosorbent was washed several times with distilled water in order to remove excess acid and used for next biosorption cycle. The biosorption and desorption procedures were repeated using the same biosorbent.

3. Results and Discussion
3.1 Characterization of biosorbents

All fresh and treated BSF were composed mainly of cellulose, hemicellulose and lignin (Table 1). BSF-raw possessed lowest fraction of cellulose content and highest fraction of hemicellulose and lignin contents. While, NaOH treatment increased the fraction of cellulose content from

58.21% to 65.73% and decreased the fraction of hemicellulose and lignin contents by about 6.5% and 1.1%, respectively. Similarly, HCl treatment extensively altered the composition of BSF with the fractions of cellulose, hemicellulose and lignin contents were 88.3%, 6.98% and 4.71%, respectively.

The X-ray diffraction (XRD) patterns of BSF adsorbents are shown in Fig. 1A. The XRD patterns of all BSF exhibited mainly the cellulose *I* structure which consists of two distinct crystal phases, namely I_α and I_β. The major peak at $2\theta = 21.9°$ corresponds to the crystalline structure of cellulose *I*, whilst the amorphous background is characterized by the low diffracted intensity at a shoulder peak in the region $2\theta = 14\text{-}16°$. The crystallinity indices of BSF-raw, BSF-HCl and BSF-NaOH were 66.3%, 64.4%, and 71.8%, respectively (Table 1). These results demonstrated that the crystallinity of adsorbent progressively increases after alkali treatment due to progressive removal of amorphous hemicellulose and lignin.[23] At higher crystallinity, the cellulose molecules are arranged in ordered lattice and most of OH groups were bonded by hydrogen bond (C–H⋯O). In contrast, the acid treatment decreased the crystallinity index showing the destroying of the hydrogen bonding groups.[24] Similarly, Dafalla et al. reported that the acidic treatment of rice husk is one of the most effective reagents for structural break-down or removal of lignin and hemicellulose thus reduce the cellulose crystallinity.[25]
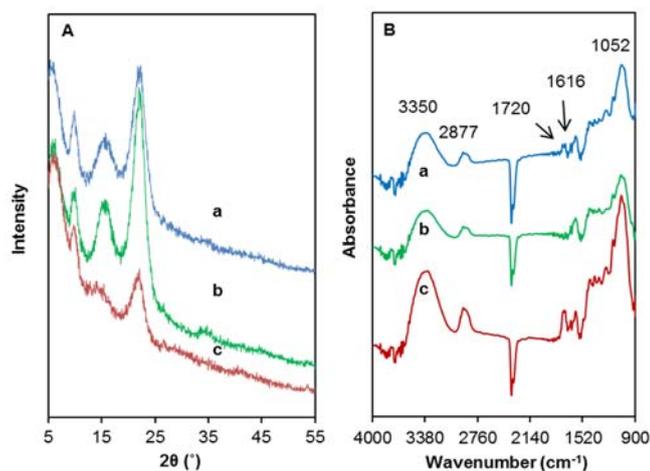

Fig.1 A) XRD and B) FTIR spectra of a) BSF-raw, b) BSF-NaOH and c) BSF-HCl

Fig. 1B illustrates the FTIR spectra of activated BSF adsorbents. All BSF adsorbents possessed an absorbance bands centered at 3350 and 2877cm^{-1} corresponding to OH groups from the glucosidic ring of cellulose and C–H stretching of the methyl and methylene groups.[26] The small absorbance bands at 1720 and 1616 cm^{-1} are ascribed to vibrational stretching of unconjugated C=O mainly due to aliphatic carboxylic acids/ketone from hemicellulose groups and conjugated carbonyl present in typical lignin groups. While, in the region of 1030-1150 cm^{-1}, the absorbance bands, the absorbance bands mainly attributed to the carbohydrates (cellulose and lignin)

including C-O-C and C-O stretching bands.[27] In general, the intensity of the bands decreased by alkali treatment. However, the bands were intensified after acid treatment due to the collapsing of the chemical bonding of BSF resulting in higher number of active sites. Particularly, the band at 1720 cm^{-1} was almost eliminated by alkaline treatment. The resulting spectra essentially contained typical lignocellulosic fibres band which similar to the previous studies on sugarcane bagasse, weeds, mustard husk, sponge gourd and coconut.[10,28-30]

Table 1 Chemical composition of BSF-raw, BSF-NaOH and BSF-HCl.

Biosorbent	Cellulose (%)	Hemicellulose (%)	Lignin (%)	X_c (%)
BSF-raw	58.21	26.95	14.83	66.3
BSF-NaOH	65.73	20.5	13.76	64.4
BSF-HCl	88.3	6.98	4.71	71.6

3.2 Biosorption of Hg(II)

3.2.1 Effect of activation, treatment and contact time

Fig. 2A illustrates the Hg(II) biosorption capacity of BSF in the effect of treatment, activation and contact time. Similar trend was observed on both fresh and activated BSF in which the biosorption rate increased rapidly at initial stage and then decreased to some extent. The equilibrium achieved at 90 and 180 min for fresh and activated BSF, respectively. Therefore, 180 min was used for all further equilibrium studies in this report unless otherwise mentioned. The highest equilibrium uptake was achieved on activated BSF-HCl with 15 mg g^{-1}, followed by activated BSF-NaOH (12 mg g^{-1}) and activated BSF-raw (9.8 mg g^{-1}). The highest Hg(II) biosorption for activated BSF-HCl may be due to the lowest crystallinity index of BSF-HCl which led to increase in the accesibility of metal ion sorbate to the cellulose. Whereas, the biosorption capacity of fresh BSF did not typically exceed 1.8 mg g^{-1}. The low biosorption capacity may be due to a low concentration of structural defect and/or electron deficient oxygen as indicated by the relative intensities of the FTIR bands in Fig. 2B and ESR signal in Fig. 3.

The effect of BSF-HCl activation on the Hg(II) biosorption is portrayed by FTIR analysis in Fig. 2B. The activation of BSF-HCl decreased the absorbance bands at 3350 and 1616 cm^{-1} indicating the abstraction of OH group and/or hydrogen atom from the hydroxyl group on the cellulose (Fig. 2B,c). Fig. 2B,b and 2B,d show the interaction of Hg(II) with fresh and activated BSF-HCl. The decrease in the intensity of the bands at 3350, 2877, 1720 and 1052 cm^{-1} confirmed the interaction of Hg(II) with the hydroxyl and/or carboxyl groups in the BSF. However, almost no interaction was observed in the band at 1616 cm^{-1} revealing that the conjugated carbonyl in the lignin groups has no ability to adsorb Hg(II). The Hg(II) biosorption at 3350 and 1052 cm^{-1} was extensively observed on activated
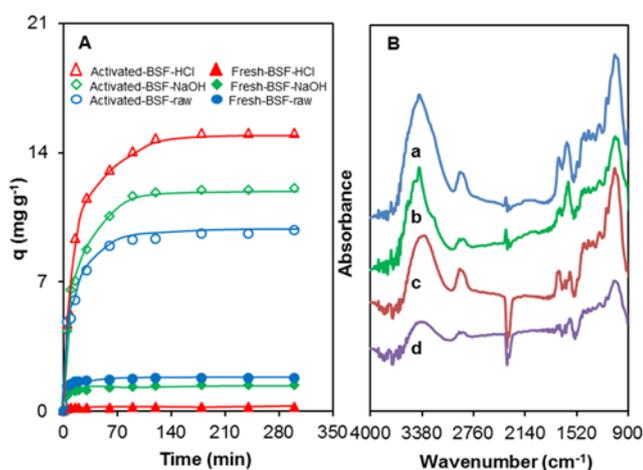
Fig. 2 A) Effect of treatment and activation of BSF on the biosorption of Hg(II) [initial Hg(II) concentration: 10 mg L^{-1}; mass dosage: 0.08 g, pH =7, temperature= 303 K] and B) FTIR spectra of a) Fresh BSF-HCl, b) Hg adsorbed on fresh BSF-HCl, c) Activated BSF-HCl and d) Hg adsorbed on activated BSF-HCl (Hg-BSF-HCl).

Fig. 3 A) Thermogravimetry and B) ESR analyses of fresh activated BSF-HCl and Hg-BSF-HCl.

BSF-HCl showing the activation process generated surface defects which led to interact with Hg(II).

Fig. 3 shows the thermogravimetric and ESR analyses of activated BSF-HCl and Hg adsorbed on activated BSF-HCl (denote as Hg-BSF-HCl). In Fig. 3A, the initial 5 wt% weight loss below 373 K for both samples was caused by water evaporation or removal of structurally bound water molecules. Activated BSF-HCl presented a thermal stability in the range of 373-473 K. At 573-773 K, both samples showed a considerable mass loss due to the decomposition of cellulose and hemicellulose and degradation of protolignin in the fibers. However, at 773 K and above, the char yield of Hg-BSF-HCl is higher than that of activated BSF-HCl due to the presence of mercury species. This result is similar with the char yield of aminated chelating fiber (AF) loaded with Hg ions which the Hg-adsorbed AF was weigher than the fresh AF.[31] The presence of Hg(II) ions on activated BSF-HCl was also observed in the ESR signal. The change in the intensity of ESR signal in Fig. 3B exhibited a simultaneous evidences of the surface defects (electron deficient oxygen) availability and interaction of the surface defects with Hg(II) ions.[32] As the BSF-HCl was activated at 373 K for 1 h, the intensity of the ESR signal corresponding to an electron deficient oxygen at g=1.9809 increased indicating the presence of more electron deficient oxygen resulting from the abstraction of hydrogen atom from the hydroxyl group on carbon of the cellulose.[33-34] The Hg(II) biosorption on activated BSF-HCl shifted the g-factor to a lower value of 1.9804 showing the Hg(II) ion interacted with electron deficient oxygen of the biosorbent.

The surface morphology of fibers can be undertaken by observation of FESEM images (Fig. S1). The surface structure of untreated BSF and BSF-raw were rough and irregular. However after alkali or acid treatment, the presence of re-
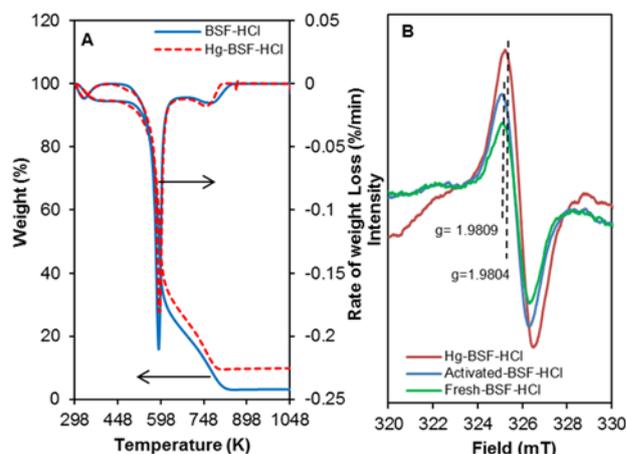
latively well organized, pronounced and uniform cavities distributed around the surface, indicated a good possibility for the metal ions to be adsorbed.[35] Although no significant difference was observed in the FESEM images of fresh BSF-HCl and Hg-BSF-HCl, the EDX spectrum showed the presence of peak corresponding to Hg element on the Hg-BSF-HCl.

3.2.2 Effect of pH

pH of the solution strongly affects the surface structure of adsorbents and the formation of transition metal ions which led to affect in the interaction between adsorbents and transition metal ions and stability of the formed metal complexes. The pH$_{zpc}$ of the Hg(II) biosorption on activated BSF-HCl is at 5.8, and the surface charge of the biosorbent is positive below this pH$_{zpc}$ and negative above this pH$_{zpc}$ (Fig. S2-A). At pH less than pH$_{zpc}$ the predominant species [M^{n+} and M(OH)$^{(n-1)+}$] are positively charged therefore the metals uptake in the pH range of 2-5 is a H$^+$–M^{n+} exchange process which also known as an electrostatic repulsion phenomenon. Thus, Hg(II) biosorption on activated BSF-HCl at acidic pH may be inefficient due to competition between the hydronium ions and the positively charged Hg ions for the surface adsorbing sites; subsequently biosorption of mercury ions may be low. At above pH$_{zpc}$, biosorption capacity of activated BSF-HCl may be higher due to the increase in the electrostatic attraction between positive sorbate species and negatively surface charged adsorbent. The Hg(II) biosorption on activated BSF-HCl increased with the pH and reached maximum capacity at pH 7 (Fig. S2-B). However, at higher pH values, the Hg(II) biosorption decreased which may be due to the formation of soluble hydroxyl complexes.[13,36]

3.3 Isotherm studies

The equilibrium data were analyzed using linear and non-linear regression method of two- and three-parameter models in order to examine the relationship between adsorption and aqueous concentration at equilibrium. The two-parameter

isotherm model is Langmuir, Freundlich and Temkin; whereas the three-parameter model is Redlich-Peterson, Koble-Corrigan and Sips (Table S1).

The applicability of the experimental data in fitting the equation isotherm models were determined by regression coefficient, R^2 and error function. Marquadt's percent standard deviation was employed as the error function and is given as below;

$$MPSD = 100 \times \left(\sqrt{\frac{1}{p-n} \sum_{i=1}^{p} \left[\frac{(q_{e,meas} - q_{e,calc})}{q_{e,meas}} \right]_i^2} \right) \quad (2)$$

where p is the number of experiments and n is the number of parameters of a model equation. The adsorption capacity from the experimental data and from the model equation were denoted as $q_{e,meas}$ and $q_{e,calc}$, respectively. In the error estimation, the lower the MPSD value indicates better fit of the isotherm equations.[35] The coefficients and MPSD error values for all isotherm models are listed in Table 2.

3.3.1 Two-parameter isotherm

Freundlich isotherm describes non-ideal and reversible adsorption, not restricted to the formation of monolayer. This empirical model can be applied to multilayer adsorption, with non-uniform distribution of adsorption heat and affinities over the heterogeneous surface. The experimental data for both fresh and activated BSF-HCl fitted the linear and non-linear form of Freundlich isotherm satisfactorily with R^2 value ranging from 0.932 to 0.977 ((Fig. S3-A and S3-D); Fig 4A and 4B; Table 2). The value of n, of this model, falling in the range of 1-10 indicates favorable adsorption.

The Langmuir model is based on the assumption that the maximum adsorption occurs when a saturated monolayer of solute molecules present on the adsorbent surface, the energy of adsorption is constant and there is no migration of adsorbate molecules in the surface plane. It is served to estimate the maximum metal uptake values where they could not be reached in the experiments. It contains two constant parameters where q_m is the maximum biosorption capacity reflected a complete monolayer and K_L is a constant that represents affinity between the sorbent and sorbate. The experimental data fitted very well with Langmuir model indicating monolayer surface adsorption taken place in the adsorption ((Fig. S3-B and S3-E); Fig. 4A and 4B; Table 2). The maximum biosorption capacity, q_m value was 269 and 372 mg g⁻¹ for activated BSF-HCl using linear and non-linear method, respectively. This value is better than the fresh BSF-HCl and other adsorbents reported in the literature (Table 5). It is about 4-fold higher than carboxyl banana stem reported by Anirudhan et al. and it is more than sixteen-fold higher than raw rice straw.[13-36] The R_L value were in the range 0.699 to 0.944 showing that Hg(II) biosorption onto BSF-HCl is favorable. In contrast, low R^2 values were obtained for Temkin isotherm for fresh BSF-HCl (0.847) and activated BSF-

HCl (0.939) when compared with the other two-parameter models. Hence, the experimental data could not be described by Temkin model.

3.3.2 Three-parameter isotherm

The Redlich–Peterson equation incorporates features of Langmuir and Freundlich isotherm models. It approaches the Freundlich model at high concentration and is in accord with the low concentration limit of the Langmuir equation. The constant g characterizes the isotherm as: if $g=1$, the Langmuir will be the preferable isotherm, while if $g=0$, the Freundlich isotherm will be the preferable isotherm. It is worth noting that g value was close to unity for Hg(II) biosorption on fresh and activated BSF-HCl, i.e., the data can preferably be fitted with Langmur model. This is confirmed by the satisfactory fit of the data to Langmuir model with R^2, 0.968 and 0.994 for fresh and activated BSF-HCl, respectively (Fig. 4A and 4B; Table 2). Furthermore, this model had the best fit with the experimental data due to the lowest MPSD value (MPSD= 17.2) for activated BSF-HCl compared to other isotherm models.

Similarly, Koble-Corrigan model is also a three parameters empirical model which combined both Langmuir and Freundlich isotherm equations in a one non-linear equation for representing the equilibrium biosorption data. Based on the n value of 1, this model indicates the favorable of Langmuir model over Freundlich model. Hence, the monolayer Hg(II) biosorption onto fresh and activated BSF-HCl is preferable.

The Sips isotherm model, known as Langmuir-Freundlich isotherm which inferred for predicting the heterogeneous adsorption system and circumventing the limitation of the rising adsorbate concentration associated with Freundlich isotherm model. At low adsorbate concentrations, it reduces to Freundlich isotherm; while at high concentrations, it predicts a monolayer adsorption capacity characteristic of the Langmuir isotherm. The value of Sips isotherm constant, m_S were both approaching or equal 1 suggesting that the isotherm is approaching Langmuir instead of Freundlich.

Based on the experimental fitting data, the best isotherm models fitted for Hg(II) biosorption on fresh and activated BSF-HCl were determined in the order of Redlich-Peterson > Koble-Corrigan > Sips > Langmuir > Freundlich > Temkin. It is also suggested that the three-parameter models resulted a better fitting than those of two-parameter models. Since the Redlich-Peterson parameter g is unity, this means that the equilibrium isotherm behaves as a Langmuir. Thus it can be concluded that the Hg(II) biosorption on activated BSF-HCl is applicable to monolayer (chemisorption) adsorption.

3.4 Kinetic studies

In order to clarify the biosorption kinetics of Hg(II) onto fresh and activated BSF-HCl, two kinetic models, which are Lagergren's pseudo-first-order[37] and Ho pseudo-second-order models[38] were applied. Moreover, linear and non-linear regression methods were compared to determine the best fitting

Table 2 Parameters of isotherm study for the Hg(II) biosorption on BSF-HCl at different Hg(II) initial concentration [mass dosage= 0.01 g, pH= 7, time= 3h, temperature= 303 K].

Fresh BSF-HCl					Activated BSF-HCl				
Two-parameters Isotherm Model	Parameter		Three-parameters Isotherm Model	Parameter	Two-parameters Isotherm Model	Parameter		Three-parameters Isotherm Model	Parameter
	Linear	Non-linear		Non-linear		Linear	Non-linear		Non-linear
Freundlich			**Redlich-Peterson**		**Freundlich**			**Redlich-Peterson**	
n	1.6	2.2	A	0.189	n	1.3	1.8	A	9.9 x10⁻⁵
K_f	3.7	3.2	B	1.9	K_f	64.9	15.8	B	3.4
R_2	0.94	0.977	g	1	R_2	0.969	0.932	g	1
MPSD		57.3	R^2	0.968	MPSD		58.7	R^2	0.994
			MPSD	44.2				MPSD	17.2
Langmuir			**Koble-Corrigan**		**Langmuir**			**Koble-Corrigan**	
q_m	9.2	28	A	1.8	q_m	269	372	A	0.624
K_L	0.333	0.046	n	1	K_L	0.017	0.013	n	1
R_L	0.699	0.944	B	0.048	R_L	0.922	0.938	B	0.002
R^2	0.951	0.964	R^2	0.967	R^2	0.980	0.979	R^2	0.994
MPSD		39.4	MPSD	41.9	MPSD		25.6	MPSD	36.2
Temkin			**Sips**		**Temkin**			**Sips**	
A	1.5	1.6	q_{mS}	1.8	A	0.209	0.209	q_{mS}	312
B	633.7	3.9	m_S	1	B	37	68.2	m_S	1
R^2	0.837	0.847	K_S	0.048	R^2	0.939	0.939	K_S	0.002
MPSD		282	R^2	0.967	MPSD		94.6	R^2	0.994
			MPSD	41.9				MPSD	36.2

of kinetic model to experimental data.

The pseudo-first-order kinetic equation based on adsorption equilibrium capacity is expressed in the following form:

$$q_t = q_e\left(1 - e^{-k_1 t}\right)$$

(3)

while the pseudo-second-order kinetic model can be written in the following form:

$$q_t = \frac{q_e^2 k_2 t}{1 + q_e k_2 t}$$

(4)

where q_t and q_e (mg g⁻¹) are the amounts of the Hg(II) ions adsorbed at time t and equilibrium, respectively, while k_1 (min⁻¹) and k_2 (g mg⁻¹ min⁻¹) are pseudo-first-order and pseudo-second-order rate constants, respectively. Furthermore, Equation (4) can be rearranged and further linearized as;

$$\log(q_e - q_t) = loq(q_e) - \frac{k_1 t}{2.303}$$

(5)

while the linear form of pseudo-second order can be expressed as;

$$\log(q_e - q_t) = loq(q_e) - \frac{k_1 t}{2.303}$$

(6)

while the linear form of pseudo-second order can be expressed as;

$$\frac{t}{q_t} = \frac{1}{k_2 q_e^2} + \frac{1}{q_e} t$$

(7)

The values of rate constants for both models as well as the corresponding correlation coefficient value (R^2) were determined at different temperatures (Table 3). In all conditions studied, the values of R^2 for the pseudo-second order models were greater than the pseudo-first-order models for both fresh and activated BSF-HCl (Fig. S4; Fig. 4C & 4D). In addition, the theoretical $q_{e2,cal}$ values were closer to the experimental $q_{e,exp}$ values. These results provided evidences that the pseudo-second-order kinetics model could be more precise fit of kinetic data to represent the Hg(II) biosorption kinetic on the BSF-HCl. Therefore, it is suggested that the Hg(II) biosorption over BSF-HCl is controlled by chemisorption process. Similar phenomenon was reported by Tuzen et al. where the kinetic be-

Table 3 Parameters of kinetic study for the Hg(II) biosorption on BSF-HCl at different temperatures [initial Hg(II) concentration= 100 mg L^{-1}, mass dosage= 0.01 g, pH= 7, time= 3h].

| T (K)	$q_{e,exp}$ mg g^{-1}	Pseudo-first-order						Pseudo-second-order					
		Linear			Non-linear			Linear			Non-linear		
		k_1 min^{-1}	$q_{e,calc}$ mg g^{-1}	R^2	k_1 min^{-1}	$q_{e,calc}$ mg g^{-1}	R^2	k_2 g mg^{-1} min^{-1}	$q_{e,calc}$ mg g^{-1}	R^2	k_2 g mg^{-1} min^{-1}	$q_{e,calc}$ mg g^{-1}	R^2
Fresh BSF-HCl													
303	2.8	0.051	1.4	0.959	0.193	2.6	0.983	0.111	2.8	0.999	0.098	2.8	0.998
308	2.4	0.044	1.2	0.944	0.229	2.2	0.959	0.157	2.4	0.988	0.094	2.5	0.999
313	2.2	0.048	1.4	0.84	0.229	2	0.952	0.171	2.1	0.979	0.077	2.3	0.996
323	2.1	0.052	1.5	0.824	0.172	1.9	0.96	0.129	2	0.985	0.077	2.1	0.995
Activated BSF-HCl													
303	215	0.058	200.9	0.974	0.075	210.7	0.987	0.0004	233.8	0.989	0.0004	228	0.998
308	94.5	0.035	45.3	0.929	0.131	91.2	0.986	0.002	97.5	0.999	0.002	97	0.999
313	45	0.042	27.3	0.958	0.139	42.8	0.973	0.004	45.7	0.997	0.004	46	0.999
323	28	0.036	20.8	0.959	0.076	26.8	0.991	0.003	29	0.993	0.003	29	0.999
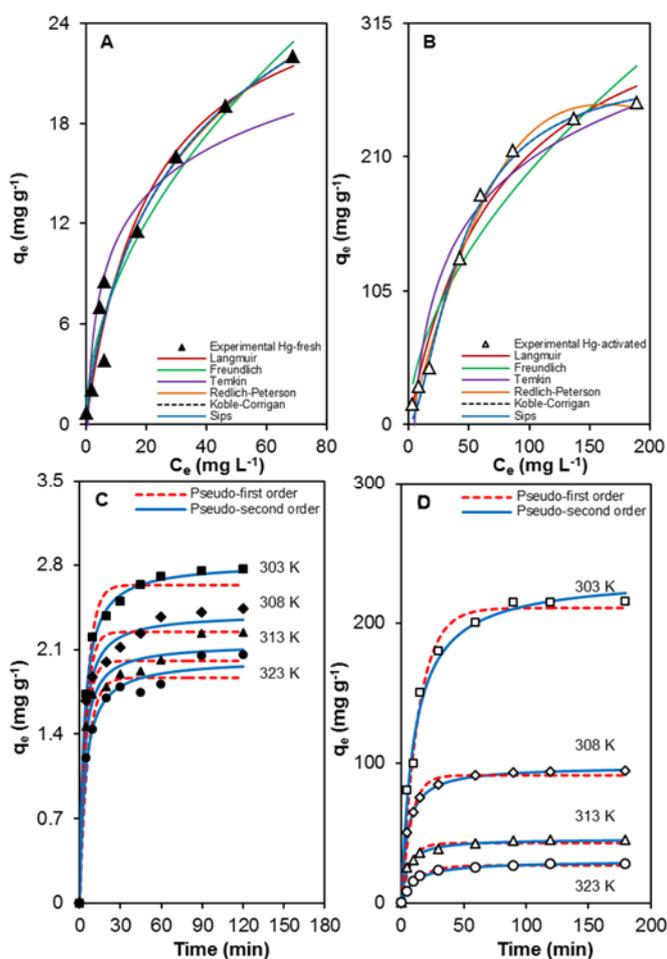
Fig. 4 Biosorption isotherms for the Hg(II) biosorption onto A) fresh BSF-HCl and B) activated BSF-HCl at different initial Hg(II) ions concentration and kinetics of the biosorption of Hg(II) onto C) fresh BSF-HCl and D) activated BSF-HCl at different temperatures using non-linear method

haviour of Hg(II) biosorption using lichen (*Xanthoparmelia conspersa*) biomass was predicted as chemical sorption being the rate-controlling step, due to high R^2 values (0.991-0.997) and the theoretical $q_{e2,cal}$ values were closer to the experimental $q_{e,exp}$ values obtained from pseudo-second order model.[39] Apart from that, the results for linear and non-linear regression methods are close to each other but non-linear exhibited higher coefficient of determination values for kinetic analysis than the linear regression (Table 3).

To study the nature of the diffusion process of the Hg(II) ions from the solution to the surface of the biosorbent, the kinetic data obtained was modelled through Weber-Morris intra-particle diffusion model[40] given by the following expression:

$$q_t = k_{id} d^{1/2} + C \tag{8}$$

where q_t is the amount of Hg(II) adsorbed at a given time t, k_{id} is the intraparticle diffusion constant and C is the intercept. As can be observed in Fig. 5, the plots are not linear over the whole time range and, instead, can be separated into three or two-linear curves, illustrating that more than one stages were involved in the adsorption process. Both fresh and activated BSF-HCl undergoes three steps at temperature 303 K while two steps were involved when temperature increased above 303 K. Since the first linearity slope is larger than that of the second, hence the first step, being the external surface adsorption correlated to the boundary layer diffusion, is faster than the second assigned to the intra-particle diffusion. Accordingly, this latter is greatly concerned in the rate control of this mechanism. At 303 K, the last linearity is attributed to the equilibrium stage. By looking at the second linearity, we can easily notice that it does not pass by the origin, which points out that the intra-particle diffusion is not the only rate determining step and confirmed that the process is chemisorptions.[41]
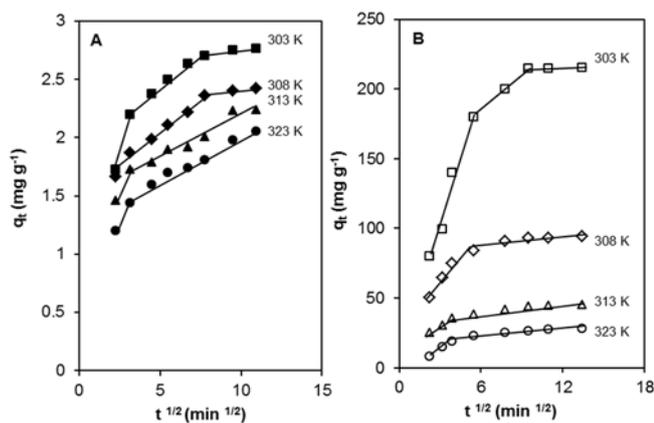
Fig. 5 Intra-particle diffusion models for Hg(II) biosorption onto A) fresh BSF-HCl and B) activated BSF-HCl.

3.5 Thermodynamic studies

The effect of temperature on the Hg(II) biosorption efficiency from aqueous solutions using fresh and activated BSF-HCl was studied at 303-323 K (Fig. S5-A and S5-B). Decreasing trend in Hg(II) biosorption capacity with an increase in the temperature indicated the process to be an exothermic. This phenomenon may be physical in nature and usually occurs as a result of Van der Waals forces between adsorbent and adsorbate. In such a case the adsorbed molecule is not fixed to a specific site at the surface but is free to undergo translational motion at the interface.

The temperature dependence of adsorption is associated with various thermodynamic parameters. The thermodynamic parameters such as free energy ($\Delta G°$), enthalpy ($\Delta H°$) and entropy ($\Delta S°$) change of adsorption can be evaluated from the following Eq. (9) to Eq. (12):

$$K_c = \frac{C_{Ae}}{C_e} \tag{9}$$

$$\Delta G° = -RT \ln K_c \tag{10}$$

$$\Delta G° = \Delta H° - T\Delta S° \tag{11}$$

$$\ln K_c = \frac{\Delta S°}{R} - \frac{\Delta H°}{RT} \tag{12}$$

where K_c is the equilibrium constant, C_e is the equilibrium concentration in solution (mg L^{-1}) and C_{Ae} is the amount of Hg(II) adsorbed on the adsorbent per liter of solution at equilibrium (mg L^{-1}). $\Delta G°$, $\Delta H°$ and $\Delta S°$ are changes in Gibbs free energy (kJ mol^{-1}), enthalpy (kJ mol^{-1}) and entropy (J mol^{-1}

K^{-1}), respectively. R is the gas constant, T is the temperature (K).

The negative values of $\Delta G°$ obtained at all temperatures for fresh BSF-HCl (-4.4, -2.7, -1.9 and -0.9 kJ mol^{-1}) indicated that the Hg(II) biosorption is spontaneous. In contrast, the positive values of $\Delta G°$ for activated BSF-HCl (5.2, 7.7, 9.8 and 11.4 kJ mol^{-1}) illustrated the non-spontaneity in nature. While, the $\Delta H°$ and $\Delta S°$ parameters can be calculated from the slope and intercept of the plot of ln K_c vs 1/T yields, respectively (Fig. S5-C). The negative values of $\Delta H°$ and $\Delta S°$ for Hg(II) biosorption obtained on both fresh BSF-HCl and activated BSF-HCl confirms the exothermic nature of the biosorption process and a decrease in the randomness at the solid/solution interface, respectively (Table 4). Similarly, Anirudhan et al. studied that adsorption of polyacrylonitrile grafted banana stem having carboxylate functional groups (CBS) on Hg(II) ions is an exothermic process.[36] They reported that this phenomenon can be explained by the fact that Hg(II) ions are bound to carboxylate functional groups via Van der Waals binding to the adsorbent surface.

The activation energy (E_a) is defined as the minimum kinetic energy required by the adsorbate ions to react with the active sites available on the surface of the biosorbent. The value of E_a can be obtained by the general Arrhenius equation.[42] The E_a value obtained from the slope of the plot of ln k_2 vs 1/T was 3.5 and 76.9 kJ mol^{-1} for fresh BSF-HCl and activated BSF-HCl, respectively (Fig. S5-D and Table 4). Thus, it can be concluded that the Hg(II) biosorption onto fresh BSF-HCl is a physisorption process due to low E_a value. However, the activation increased the E_a and changed the physisorption to chemisorption process.[41] Based on the kinetic and thermodynamic studies, both physisorption and chemisorption processess occured during Hg(II) biosorption onto BSF-HCl. This may be due to the ability of activated BSF-HCl to interact by both electrostatic interactions and chemically binding with the Hg(II) ions on the surface of biosorbent. In fact, the activated BSF-HCl possesses higher concentration of structural defects and/or oxygen radicals which led to interact with Hg(II) ions to form chemical bonding.

Table 4 Thermodynamic parameters for the Hg(II) biosorption on BSF-HCl at different temperatures [initial Hg(II) concentration= 100 mg L^{-1}, mass dosage= 0.01 g, pH= 7, time= 3h].

Biosorbent	T (K)	$\Delta G°$ (kJ mol^{-1})	$\Delta H°$ (kJ mol^{-1})	$\Delta S°$ (J mol^{-1}K^{-1})	E_a (kJ mol^{-1})
Fresh BSF-HCl	303	-4.4	-54.3	-166.2	3.5
	308	-2.7			
	313	-1.9			
	323	-0.9			
Activated BSF-HCl	303	5.2	-86.4	-304.4	76.9
	308	7.7			
	313	9.8			
	323	11.4			

3.6 Comparison with other adsorbents

The maximum Hg(II) biosorption capacity (q_m) on BSF-HCl and other adsorbents reported in the literature are given in Table 5. The result indicated the maximum biosorption capacity of activated BSF-HCl in this study is 372 mg g^{-1}. This value was higher than the maximun capacity of other low-cost adsorbents. Previously, Anirudhan et al. reported that coconut coir pith was found to have good adsorption capacity (160 mg g^{-1}) due to substance inherently associated with cellulose.[14] The presence of polyphenolic and aliphatic hydroxyl and carboxylic groups on cellulose will apparently attract the Hg(II) ions. Orlando et al. studied the removal of Hg using modified sugarcane.[43] In their study, the sugarcane bagasses were converted to effective chelating agents by reaction with urea under microwave irradiation. This modification displayed an excellence result with maximum adsorption capacity of 280 mg g^{-1}; however it needs longer time to achieve equilibrium. The easy availability and cost effectiveness of BSF-HCl are some of the additional advantages, reflecting a promising future for BSF utilization in mercury(II) removal from aqueous solutions.

Table 5 Comparison of BSF-HCl with other adsorbents for Hg(II) biosorption.

Adsorbent	Heavy metal	Contact time (h)	pH	q_m (mg g^{-1})	Ref.
Activated BSF-HCl	Hg	3	7	372	This study
Fresh BSF-HCl	Hg	1.5	7	28	This study
Carboxyl banana stem	Hg	3	6-9	90.9	36
Coir pith	Hg	3	6	160	14
Urea-sugarcane bagasse	Hg	24	6	280	43
Sago waste	Hg	1.75-2	5	55.6	44
Rice straw	Hg	1.5	5	22.1	13

3.7 Reuse of the biosorbent

Desorption and regeneration studies were carried out using 50 mL 0.1 M HCl as eluted solution. The biosorbent was washed with water before each measurement. The results in Table S2 clearly shows that BSF-HCl can be used repeatedly without significantly loosing its adsorption capacity for Hg(II). After four cycles, the Hg(II) biosorption capacity decreased from 95.2 to 85.2 %. This behaviour indicated that BSF-HCl can be used successfully four times after regeneration for the removal of Hg(II).

4. Conclusion

This study demonstrated the utilization of activated BSF-HCl for efficient biosorption of Hg(II). HCl treatment and heating in vacuo at 373 K markedly increased the cellulose accessibility and number of surface defects and/or oxygen radicals which induce more chemical bonding between BSF and Hg(II) ions. The kinetics of biosorption followed pseudo-second-order model with the activation energy of 76.9 kJ mol^{-1} indicating the biosorption is controlled by a chemisorption process. The equilibrium is well described by Langmuir isotherm with the maximum biosorption capacity of 372 mg g^{-1}. The thermodynamic studies provided evidence for non-spontaneity and exothermic nature of the biosorption process. Results from this study recommend that BSF-HCl is a very suitable and cost-effective biosorbent for mercury removal.

References

1 A.A. Ismaiel, M.K. Aroua and R. Yusoff, *Chem. Eng. J.*, 2013, **225**, 306.

2 X. Deng and P. Jia, *Bioresource Technol.*, 2011, **102**, 3083.

3 M. Tuzen, O.D. Uluozlu, I. Karaman and M. Soylak, *J. Hazard. Mater.*, 2009, **169**, 345.

4 M. Tuzen, I. Karaman, D. Citak and M. Soylak, *Food Chem. Toxicol.*, 2009, **47**, 1648.

5 A.F. Lima, M.C. Da Costa, D.C. Ferreira, E.M. Richter and R.A.A. Munoz, *Microchem. J.*, 2015, **118**, 40.

6 M. Tuzen and M. Soylak, *Bull. Environ. Contami. Toxicol.*, 2005, **74**, 968.

7 R.K. Gautam, A. Mudhoo, G. Lofrano and M. C. Chattopadhyaya, *J. Environ. Chem. Eng.,* 2014, **2**, 239.

8 R.K. Gautam, M.C. Chattopadhyaya and S.K. Sharma, in *Waste Water Management*, ed. S.K. Sharma and R. Sanghi, Springer: London, 2013, pp 305-322.

9 R.K. Gautam, S.K. Sharma, S. Mahiya and M.C. Chattopadhyaya, in *Heavy metals in water: Presence, removal and safety*, ed. S. Sharma, RSC, London, 2014, Chapter 1, pp. 1-24.

10 L.W.S. Hoi and B.S. Martincigh, *Ind. Crop. Prod.*, 2013, **47**, 1.

11 S.S. Pillai, B. Deepa, E. Abraham, N. Girija, P. Geetha, L. Jacob and M. Koshy, *Ecotox. Environ. Safe.*, 2013, **98**, 352.

12 A.M.A. Nada, A.A. El-Gendy and S.H. Mohamed, *Carbohyd. Polym.*, 2010, **82**, 1025.

13 C.G. Rocha, D.A.M. Zaia, R.V. da Silva Alfaya and A.A. da Silva Alfaya, *J. Hazard. Mater.*, 2009, **166**, 383.

14 T.S. Anirudhan, L. Divya and M. Ramachandran, *J. Hazard. Mater.*, 2008, **157**, 620.

15 G. García-Rosales and A. Colín-Cruz, *J. Environ. Manage.*, 2010, **91**, 2079.

16 R. Mallampati and S. Valiyaveettil, *RSC Adv.*, 2012, **2**, 9914.

17 J.A. Laszlo and F.R. Dintzis, *J. Appl. Polym. Sci.*, 1994, **52**, 531.

18 N. Mosier, *Bioresource Technol.,* 2005, **96**, 673.

19 M.H. Moubasher, S.H. Abdel-Hafez and A.M. Mohanram, *J. Agr. Res.,* 1982, **46**, 467.

20 L. Segal, J.J. Creely, A.E. Martin and C.M. Conrad, *Text. Res. J.,* 1959, **29**, 786.

21 S. Triwahyono, T. Yamada, H. Hattori, *Catal. Lett.,* 2003, **85**, 109.

22 A. Çelekli, M. Yavuzatmaca and H. Bozkurt, *Chem. Eng. J.,* 2009, **152**, 139.

23 M. Sheltami, I. Abdullah, I. Ahmada, A. Dufresnec and H. Kargarzadeh, *Carbohyd. Polym.,* 2012, **88**, 772.

24 L. Zheng, C. Zhu, Z. Dang, H. Zhang, X. Yi and C. Liu, *Carbohyd. Polym.*, 2012, **90**, 1008.

25 S.B. Dafalla, H. Mukthar and M.S. Shaharum*, Inter. J. Chem. Environ. Eng.*, 2012, **3**, 3.

26 J.L. Guimarães, E. Frollini, C.G. da Silva, F. Wypych and K.G. Satyanarayana, *Ind. Crop. Prod.*, 2009, **30**, 407.

27 V.K. Gupta and A. Rastogi, *J. Hazard. Mater.*, 2009, 163, 396.

28 R.K. Gautam, A. Mudhoo and M.C. Chattopadhyaya, *J. Environ. Chem. Eng.*, 2013, **1**, 1283.

29 R.K. Gautam, P.K. Gautam, S. Banerjee, V. Rawat, S. Soni, S.K. Sharma and M.C. Chattopadhyaya, *J. Environ. Chem. Eng.,* 2014, DOI: 10.1016/J.JECE.2014.11.026.

30 R.K. Gautam, P.K. Gautam, M.C. Chattopadhyaya and J. D. Pandey, Proceedings of the National Academy of Sciences, India Section A: Physical Sciences, 2014, DOI: 10.1007/s40010-014-0154.

31 N. Ma, Y. Yanga, S. Chen and Q. Zhang*, J. Hazard. Mater.*, 2009, **171**, 288.

32 R.S. Ningthoujam, D. Lahiri, V. Sudarsan, H.K. Poswal, S.K. Kulshreshtha, S.M. Sharma, B. Bhushan and M.D. Sastry, *Mater. Res. Bull.*, 2007, **42**, 1293.

33 J.C. Arthur, J.O. Hinojosa and M.S. Bains, *J. Appl. Polym. Sci.*, 1968, **12**, 411.

34 N. Ruslan, S. Triwahyono, A.A. Jalil, S.N. Timmiati and N.H.R. Annuar, *Appl. Catal. A: Gen.*, 2012, **413**, 176.

35 K.Y. Foo, L.K. Lee and B.H. Hameed, *Chem. Eng. J.*, 2013, **223**, 604.

36 T.S. Anirudhan,P. Senan and M.R. Unnithan, *Sep. Pur. Technol.*, 2007, **52**, 512.

37 S. Lagergren, *Kung. Svenska Vet. Hand.*, 1898, **24**, 1.

38 Y.S. Ho and G. Mckay, *Process Biochem.*, 1999, **34**, 451.

39 M. Tuzen, A. Sari, D. Mendil and M. Soylak, *J. Hazard. Mater.*, 2009, **169**, 263.

40 W.J. Weber and J.C. Morris, *J. Sanit. Eng. Div. Am. Soc. Civ. Eng.*, 1963, **89**, 31.

41 M.A.Z. Abidin, A.A. Jalil, S. Triwahyono, S.H. Adam and N.H.N. Kamarudin, Biochem. Eng. J., 2011, 54, 124.

42 K.J. Laidler*, J. Chem. Edu.*, 1984, **61**, 494.

43 U.S. Orlando, A.U. Baes, W. Nishijima and M. Okada, *Green Chem.*, 2002, **4**, 555.

44 K. Kadirvelu, M. Kavipriya, C. Karthika, N. Vennilamani and S. Pattabhi, *Carbon.*, 2004, **42**, 745.

RSC Advances Accepted Manuscript